

# Tuning Photoelectrochemical Performances of Ag–TiO<sub>2</sub> Nanocomposites via Reduction/Oxidation of Ag

Hao Zhang, Geng Wang, Da Chen, Xiaojun Lv, and Jinghong Li\*

Department of Chemistry, Key Laboratory of Bioorganic Phosphorus Chemistry & Chemical Biology, Tsinghua University, Beijing 100084, P. R. China

Received July 1, 2008. Revised Manuscript Received August 19, 2008

The effects of chemical states of Ag on the photoelectrochemical (PEC) properties of Ag–TiO<sub>2</sub> composites were investigated with Ag(0)–TiO<sub>2</sub> and Ag(I)–TiO<sub>2</sub> prepared by photoreduction-thermal treatment (PRT) method. The comparison of photoaction spectra of Ag(0)–TiO<sub>2</sub> and Ag(I)–TiO<sub>2</sub> showed that only the Ag(0) containing samples had notable photocurrent under visible light (in the range of 400–800 nm), which was attributed to the highly dispersed Ag(0), according to the DRS, XRD and XPS measurements. During the photocurrent spectra measurements of Ag(0)–TiO<sub>2</sub>, it was demonstrated that Ag(0) was photoexcited because of plasma resonance in the visible light region, and charge separation was accomplished by the transport of photoexcited electrons from Ag(0) to the TiO<sub>2</sub> conduction band with the simultaneous formation of Ag(I), which could be partially reduced to the initial active Ag(0) state under the following UV light irradiation. Actually, it was the interconversion of Ag(0) and Ag(I) during the alternating irradiation that avoided the rapid decay of photocurrent and ensured a durable and stable visible light-induced photocurrent. In the case of visible light degradation of methyl blue (MB), however, Ag(0)–TiO<sub>2</sub> showed poorer photocatalytic activity than Ag(I)-containing ones. It was proposed that photoexcited Ag(I) rather than Ag(0) acted as active sites that were responsible for the enhanced photocatalytic abilities, whereas Ag(0) might contribute to the stability of the photocatalysts. Hence, the Ag–TiO<sub>2</sub> nanocomposites can exhibit different photoelectrochemical performances under visible light with the different chemical states of Ag. This work could have significance not only in the mechanism study but also in the attempts to improve the visible light-induced photoactivities of Ag–TiO<sub>2</sub>, by tuning the chemical states of Ag species, in potential photoelectrochemical applications.

## 1. Introduction

Recently, there has been great interest in the photoelectrochemical (PEC) properties of nanostructured TiO<sub>2</sub> films, such as photovoltaics,<sup>1,2</sup> photocatalysis,<sup>3</sup> and water splitting.<sup>4</sup> As a promising material, TiO<sub>2</sub> has the advantages of physical and chemical stability, high activities, and low price.<sup>5–7</sup> Its main drawbacks of low quantum yield and the limited photoresponding range (usually <380 nm), however, hinder its utilizations and commercialization.<sup>3,8</sup> To handle these problems, researchers have adopted numerous strategies, including phase and morphological control, doping, sensitizations, and semiconductor coupling, etc.<sup>9–12</sup>

In particular, silver nanoparticles deposited in a TiO<sub>2</sub> film (Ag–TiO<sub>2</sub>) have attracted more and more attention because TiO<sub>2</sub> is a promising material as aforementioned and Ag is a nontoxic precious metal with remarkable catalytic activity<sup>13–16</sup> and size- and shape-dependent optical properties under visible light.<sup>17,18</sup> But because of the high activities of nano Ag as well as the diverse methods of preparation and treatment, there are debates on the chemical states of Ag in Ag–TiO<sub>2</sub>, that is to say, whether Ag(0) or Ag(I) dominates in the Ag–TiO<sub>2</sub> and plays an important role in the PEC performances. Generally, Ag(0) was considered as the main chemical state within Ag–TiO<sub>2</sub>, and the enhanced PEC properties were attributed to the surface plasma resonance (SPR) effect of metallic Ag(0) and the resulting expansion

\* Corresponding author. E-mail: jhli@mails.tsinghua.edu.cn. Tel & Fax: 86-10-62795290.

- (1) Nazeeruddin, M. K.; Kay, A.; Rodicio, I.; HumphryBaker, R.; Muller, E.; Liska, P.; Vlachopoulos, N.; Gratzel, M. *J. Am. Chem. Soc.* **1993**, *115*, 6382–6390.
- (2) O'Regan, B.; Gratzel, M. *Nature* **1991**, *353*, 737–739.
- (3) Hoffmann, M. R.; Martin, S. T.; Choi, W.; Bahnemann, D. W. *Chem. Rev.* **1995**, *95*, 69–96.
- (4) Bard, A. J.; Fox, M. A. *Acc. Chem. Res.* **1995**, *28*, 141–145.
- (5) Fujishima, A.; Honda, K. *Nature* **1972**, *238*, 37–38.
- (6) Robel, I.; Subramanian, V.; Kuno, M.; Kamat, P. V. *J. Am. Chem. Soc.* **2006**, *128*, 2385–2393.
- (7) Suzuki, M.; Ito, T.; Taga, Y. *Appl. Phys. Lett.* **2001**, *78*, 3968–3970.
- (8) Hu, C.; Lan, Y.; Qu, J.; Hu, X.; Wang, A. *J. Phys. Chem. B* **2006**, *110*, 4066–4072.
- (9) Carp, O.; Huisman, C. L.; Reller, A. *Prog. Solid State Chem.* **2004**, *32*, 33–177.
- (10) Wang, G.; Lu, W.; Li, J. H.; Choi, J.; Jeong, Y.; Choi, S. Y.; Park, J. B.; Ryu, M. K.; Lee, K. *Small* **2006**, *2*, 1436–1439.

- (11) Zhao, W.; Ma, W. H.; Chen, C. C.; Zhao, J. C.; Shuai, Z. G. *J. Am. Chem. Soc.* **2004**, *126*, 4782–4783.
- (12) Chen, D.; Zhang, H.; Hu, S.; Li, J. H. *J. Phys. Chem. C* **2008**, *112*, 117–122.
- (13) Guin, D.; Manorama, S. V.; Latha, J. N. L.; Singh, S. *J. Phys. Chem. C* **2007**, *111*, 13393–13397.
- (14) Hermann, J. M.; Tahiri, H.; Ait-Ichou, Y.; Lossaletta, G.; Gonzalez-Elipe, A. R.; Fernandez, A. *Appl. Catal., B* **1997**, *13*, 219–228.
- (15) Vamathevan, V.; Amal, R.; Beydoun, D.; Low, G.; McEvoy, S. *J. Photochem. Photobiol. A* **2002**, *148*, 233–245.
- (16) Arabatzis, I. M.; Stergiopoulos, T.; Bernard, M. C.; Labou, D.; Neophytides, S. G.; Falaras, P. *Appl. Catal., B* **2003**, *42*, 187–201.
- (17) Ohko, Y.; Tatsuma, T.; Fujii, T.; Naoi, K.; Niwa, C.; Kubota, Y.; Fujishima, A. *Nat. Mater.* **2003**, *2*, 29–31.
- (18) Naoi, K.; Ohko, Y.; Tatsuma, T. *J. Am. Chem. Soc.* **2004**, *126*, 3664–3668.

of photoresponding range.<sup>17–19</sup> But it was recently reported that Ag(0)–TiO<sub>2</sub> showed inefficiency in the photodegradation of azodyes<sup>8</sup> and decomposition of *E. coli*<sup>20</sup> under visible light, and it was also found that Ag(I) dominated within Ag–TiO<sub>2</sub>, acted as electron traps, reduced the recombination of electrons and holes, and promoted the photocatalytic activity.<sup>16,21</sup> To date, a few studies have been conducted on this debate,<sup>22–24</sup> and to some extent revealed the relation between the chemical states of Ag in Ag–TiO<sub>2</sub> and their optical properties and photocatalytic properties. However, there are still few efforts and little attention or information available on the important question that how and why the chemical states of Ag influence the PEC performances of Ag–TiO<sub>2</sub>. Thus, the effect of chemical states of Ag on different PEC performances (besides the photocatalysis) of Ag–TiO<sub>2</sub> and the corresponding mechanism, especially in the field of visible light-induced photoactivities, are still to be unraveled, not only for the theoretical purpose but also for the advance in the applications.

In this work, Ag(0)–TiO<sub>2</sub> and Ag(I)–TiO<sub>2</sub> were prepared with a photoreduction-thermal treatment (PRT) method and subsequently examined by DRS, XRD, and XPS analysis. The photocurrent action spectra of TiO<sub>2</sub> loaded with Ag in different chemical states were compared. Furthermore, possible mechanisms for electron transport and the interconversion of Ag(0) and Ag(I) induced by alternating irradiation of UV and visible light during the measurement were elucidated. Besides, the photocatalytic activities of Ag(0)–TiO<sub>2</sub> and Ag(I)–TiO<sub>2</sub> under visible light were examined with methyl blue (MB), and the effect of the chemical states of Ag was also investigated. This work will have significance in the mechanism study of Ag–TiO<sub>2</sub> nanocomposites and the enhancement of their visible light-induced PEC performances in potential applications, such as solar energy conversion, photocatalysis, and sensors.

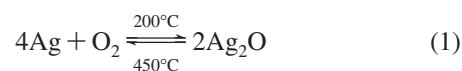
## 2. Experimental section

**2.1. Materials and Reagents.** TiO<sub>2</sub> (P25, 20% rutile and 80% anatase) was purchased from Degussa. Unless otherwise specified, AgNO<sub>3</sub>, methyl blue (MB), and other reagents and materials involved were obtained commercially from the Beijing Chemical Reagent Plant (Beijing, China) and used as received without further purification. Fluorine-doped SnO<sub>2</sub> (FTO, 15 Ω/square) glass was chosen as the electrode substrates. Ultrapure water (resistivity ≥ 18 MΩ cm) was used during the experimental process. The experiments were carried out at room temperature and humidity.

**2.2. Preparation of Ag–TiO<sub>2</sub> Films.** The Ag–TiO<sub>2</sub> nanocomposites were prepared with a photoreduction-thermal treatment (PRT) method.<sup>13,25</sup> Briefly, a suspension was prepared by mixing

P25 powder and 1 M AgNO<sub>3</sub> aqueous solution (700 mg/10 mL) in a round-bottom flask. The suspension was then irradiated with a high pressure mercury lamp (100 W) under stirring for different time (0.5/1/3/5 h). The resulting Ag–TiO<sub>2</sub> nanocomposite was recovered by filtration, rinsed with deionized water several times, and finally dried at room temperature in the dark.

The synthesized Ag–TiO<sub>2</sub> nanocomposite paste for the fabrication of photoanode was obtained by mixing ethanol and the as-prepared nanocomposite powder homogeneously (150 mg/mL). The obtained paste was spread on the FTO conducting glass with a glass rod, using adhesive tapes as spacers. After the films were dried at room temperature in dark, they were sintered at different temperatures (200 °C/450 °C) to control the chemical states of Ag in Ag–TiO<sub>2</sub>. It was demonstrated that Ag<sub>2</sub>O showed good stability at about 200 °C and totally decomposed to Ag at 450 °C.<sup>26</sup> Thus, Ag<sub>2</sub>O–TiO<sub>2</sub> (Ag(I)–TiO<sub>2</sub>) and metallic Ag–TiO<sub>2</sub> (Ag(0)–TiO<sub>2</sub>) were obtained at 200 and 450 °C, respectively, as shown in eq 1. For comparison, the pure TiO<sub>2</sub> (P25) films were prepared by spreading the TiO<sub>2</sub> paste (150 mg/mL) to FTO glass and heated at 450 °C.



**2.3. Material Characterizations.** Transmission electron microscopy (TEM) images were taken with a JEOL JEM-1010 transmission electron microscope operated at 120 kV. Diffuse reflectance spectra (DRS) of Ag–TiO<sub>2</sub> powders were recorded in the range from 200 to 800 nm using a Hitachi U-3010 spectroscopy and BaSO<sub>4</sub> was used as a reference. Powder X-ray diffraction (XRD) was performed on a Bruker D8-Advance X-ray diffractometer with monochromatic Cu Kα radiation (λ = 1.5418 Å). The 2θ range used in the measurements was from 20 to 80°. X-ray photoelectron spectra (XPS) were recorded with a PE PHI Quantera SXM microprobe system using Al Kα irradiation. All banding energies were referenced at 285.0 eV, as determined by the location of the peak C 1s spectra for the surface adventitious hydrocarbon.

**2.4. Photoelectrochemical Measurements.** The photocurrent action spectra were measured in a two-electrode home-built experimental system, where the TiO<sub>2</sub>/Ag–TiO<sub>2</sub> photoanode served as the working electrode with an active area of ca. 1 cm<sup>2</sup> and a Pt wire was used as the counter electrode in 0.1 M KNO<sub>3</sub>. A 500 W xenon lamp with a monochromator was used as the light source. The PEC cell was illuminated from the FTO side of the TiO<sub>2</sub>/Ag–TiO<sub>2</sub> photoanode electrode by incident light, and the generated photocurrent signal was collected using a lock-in amplifier (SR830 DSP, Stanford Instrument) with a light chopper (SR540, Stanford Instrument). The intensity of the monochromatic illuminating light was about 15 μW/cm<sup>2</sup> estimated with a radiometer (Photoelectronic Instrument Co. IPAS). The illumination area of the TiO<sub>2</sub>/Ag–TiO<sub>2</sub> electrode was about 0.12 cm<sup>2</sup>.

The Mott–Schottky (MS) spectra were carried out on a PARSTAT 2273 Potentiostat/Galvanostat (Advanced Measurement Technology Inc., USA) with a three-electrode cell, using the TiO<sub>2</sub>/Ag–TiO<sub>2</sub> photoanode as the working electrode, platinum wire as the counter electrode and Ag/AgCl (saturated KCl) electrode as the reference electrode in 0.1 M KNO<sub>3</sub> aqueous solution.

**2.5. Photocatalytic Measurements.** Aqueous suspensions of MB (1 × 10<sup>−5</sup> M) and the TiO<sub>2</sub>/Ag–TiO<sub>2</sub> electrodes were placed in a 3 mL quartz glass vessel. The photoreaction vessel was exposed to the visible-light irradiation under ambient conditions with an

- (19) Seery, M. K.; George, R.; Floris, P.; Pillai, S. C. *J. Photochem. Photobiol. A* **2007**, *189*, 258–263.
- (20) Elahifard, M. R.; Rahimnejad, S.; Haghighi, S.; Gholami, M. R. *J. Am. Chem. Soc.* **2007**, *129*, 9552–9553.
- (21) Sano, T.; Negishi, N.; Mas, D.; Takeuchi, K. *J. Catal.* **2000**, *194*, 71–79.
- (22) Jin, M.; Zhang, X. T.; Nishimoto, S.; Liu, Z. Y.; Tryk, D. A.; Emeline, A. V.; Murakami, T.; Fujishima, A. *J. Phys. Chem. C* **2007**, *111*, 658–665.
- (23) Zhang, L. Z.; Yu, J. C.; Yip, H. Y.; Li, Q.; Kwong, K. W.; Xu, A. W.; Wong, P. K. *Langmuir* **2003**, *19*, 10372–10380.
- (24) Zhang, L. Z.; Yu, J. C. *Catal. Commun.* **2005**, *6*, 684–687.

- (25) Zhang, F. X.; Guan, N. J.; Li, Y. Z.; Zhang, X.; Chen, J. X.; Zeng, H. S. *Langmuir* **2003**, *19*, 8230–8234.
- (26) Waterhouse, G. I. N.; Bowmaker, G. A.; Metson, J. B. *Phys. Chem. Chem. Phys.* **2001**, *3*, 3838–3845.

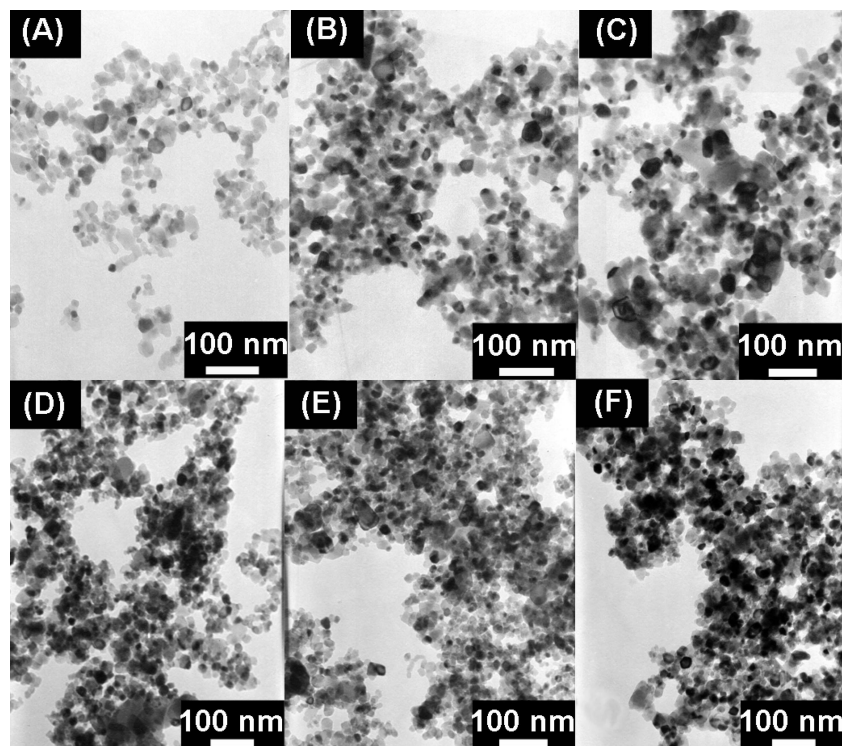


**Figure 1.** Representative TEM micrographs of (A) TiO<sub>2</sub> (P25), (B) 1 h fresh Ag–TiO<sub>2</sub>, (C) 3 h fresh Ag–TiO<sub>2</sub>, (D) 5 h fresh Ag–TiO<sub>2</sub>, (E) 3 h Ag–TiO<sub>2</sub> heated at 200 °C, (F) and 3 h Ag–TiO<sub>2</sub> heated at 450 °C nanoparticles.

average intensity of 30 mW/cm<sup>2</sup> produced by a 500 W xenon lamp with a cutoff filter ( $\lambda \geq 420$  nm), which was positioned 10 cm away from the vessel. At given time intervals, the photoreacted solution was analyzed by recording variations of the absorption band maximum (660 nm) in the UV–vis spectra of MB, using a UV–vis spectrophotometer (UV 2100, Shimadzu).

### 3. Results and Discussion

**3.1. Preparation of Ag–TiO<sub>2</sub> Nanocomposites.** The structures of TiO<sub>2</sub> (P25) and Ag–TiO<sub>2</sub> powders were examined by TEM. Figure 1A shows a representative TEM micrograph of native TiO<sub>2</sub> particles and Figure 1B–D are the micrographs of fresh Ag–TiO<sub>2</sub> samples obtained under UV light irradiation for 1, 3, and 5 h, respectively. As shown, the size and shape of the TiO<sub>2</sub> crystallites were unchanged after Ag loaded. Silver deposits with wide size-distribution were located on the surface of the individual TiO<sub>2</sub> crystallites and some Ag islands were also observed. The polydisperse and agglomerates of Ag should be attributed to its rapid overgrowth on the original TiO<sub>2</sub> particles.<sup>15,25</sup> Moreover, the loading of Ag in the nanocomposites also increased with the extension of the irradiation time, which could be further confirmed by the DRS measurement described below. In addition, images E and F in Figure 1 show the TEM images of as-prepared Ag–TiO<sub>2</sub> nanocomposites after thermal treatment at 200 and 450 °C, respectively. It was demonstrated that there were no significant changes in the size and shape of Ag before and after thermal treatment, and more agglomerates of Ag and black dots were observed for the 450 °C thermal-treated Ag–TiO<sub>2</sub> nanocomposites, which should be attributed to the accumulation and the high electron density of Ag(0) nanoparticles, respectively.

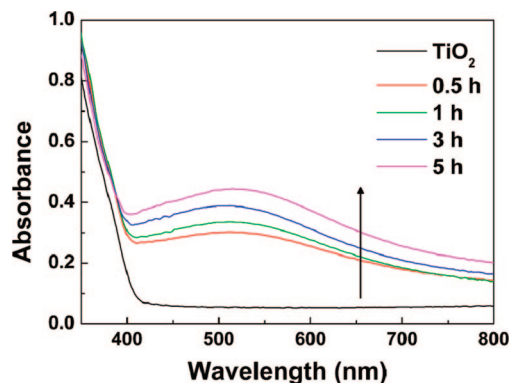


**Figure 2.** Diffuse reflectance absorption spectra of TiO<sub>2</sub> and fresh Ag–TiO<sub>2</sub> samples, from bottom to top, corresponding to the spectra of blank TiO<sub>2</sub> and fresh Ag–TiO<sub>2</sub> with the irradiation time of 0.5, 1, 3, and 5 h, respectively.

The diffuse reflectance spectra of TiO<sub>2</sub> (P25) powders and the fresh Ag–TiO<sub>2</sub> powders with irradiation time of 0.5, 1, 3, and 5 h are demonstrated in Figure 2. Compared to pure TiO<sub>2</sub>, a broad absorption covering the range of 400–800 nm with a summit at about 520 nm appeared in the spectra of Ag–TiO<sub>2</sub> nanocomposites, which should be attributed to the surface plasma resonance (SPR) effect of Ag(0). With the increase in irradiation time, the absorbance at around 520 nm increased due to the increasing amount of Ag loading. Furthermore, it is also demonstrated that compared to pure TiO<sub>2</sub>, the absorption edge of Ag–TiO<sub>2</sub> nanocomposites slightly red-shifted, which might contribute to the enhanced photoactivities under visible light.<sup>27</sup>



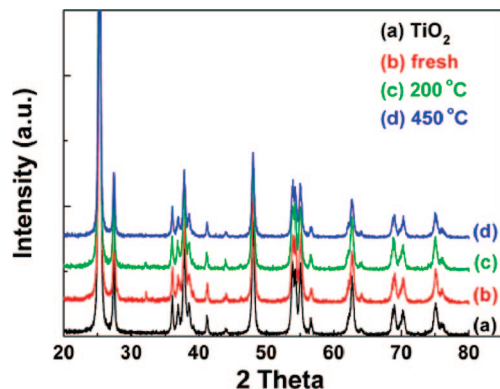


**Figure 3.** XRD patterns of  $\text{TiO}_2$  powders, fresh  $\text{Ag-TiO}_2$ , and  $\text{Ag-TiO}_2$  heated at 200 and 450  $^\circ\text{C}$ .

With the extension of irradiation time and the increase in Ag loading, the photoactivities increased first to a maximum level and then decreased, as Rengaraj et al. reported.<sup>27</sup> In our work, it was found that  $\text{Ag-TiO}_2$  with the irradiation time of 3 h had better photoactivities than others. Thus, unless otherwise specified, all the  $\text{Ag-TiO}_2$  nanocomposites discussed below were obtained with the irradiation time of 3 h.

To identify the chemical states of Ag within  $\text{Ag-TiO}_2$  before and after thermal treatment, XRD and XPS measurements were performed. Figure 3 shows the XRD patterns of pure  $\text{TiO}_2$  powders (curve a), fresh  $\text{Ag-TiO}_2$  (curve b) and the sintered  $\text{Ag-TiO}_2$  at 200 and 450  $^\circ\text{C}$  (curve c and d). All three types of  $\text{Ag-TiO}_2$  showed usual anatase and rutile phases, just like pure P25. Unexpectedly, no diffraction peaks for Ag species ( $38.1^\circ$ ,  $44.2^\circ$ ,  $64.4^\circ$ , and  $77.4^\circ$  for  $\text{Ag(0)}$ <sup>25</sup> and  $34.2^\circ$  for  $\text{Ag(I)}$ <sup>16</sup>) were observed in either  $\text{Ag-TiO}_2$  sample, which might be due to the low amount and the amorphous state of Ag.<sup>13</sup>

The corresponding XPS spectra provide further structural information for the  $\text{Ag-TiO}_2$  nanocomposites obtained, as shown in Figure 4. It can be seen that the Ti and O elements existed on the surface of pure  $\text{TiO}_2$  (curve a in Figure 4A–C), whereas Ti, O, and Ag elements occurred on the surface of the  $\text{Ag-TiO}_2$  samples. In Figure 4B, the Ag 3d spectra of  $\text{Ag-TiO}_2$  consist of two individual peaks at  $\sim 374$  and  $\sim 368$  eV, which can be attributed to Ag  $3d_{3/2}$  and Ag  $3d_{5/2}$  binding energies, respectively. The Ag  $3d_{5/2}$  peak for different  $\text{Ag-TiO}_2$  samples can be further divided into two different peaks at 368.2 and 367.7 eV, attributed to the peaks of metal Ag(0) and Ag(I) ( $\text{Ag}_2\text{O}$ ), respectively.<sup>16,28</sup> During photodeposition, most  $\text{Ag}^+$  ions in the suspension were reduced to metal Ag(0) on the  $\text{TiO}_2$  surface with a part of Ag(I) remained unreacted or came from reoxidation of photodeposited Ag in air. Thus, for the fresh  $\text{Ag-TiO}_2$ , both Ag(0) and Ag(I) were detected in XPS spectra, as shown in curve b. After the thermal treatment at 200  $^\circ\text{C}$  in air, Ag(0) deposited on the  $\text{TiO}_2$  surface was oxidized to Ag(I) ( $\text{Ag}_2\text{O}$ ), and the corresponding resolved peak at 367.7 eV for Ag(I) was also clearly observed in XPS spectra (curve c). However, the oxidized Ag(I) of  $\text{Ag-TiO}_2$  could be thermally reduced to Ag(0) during the thermal treatment at 450  $^\circ\text{C}$ , which made

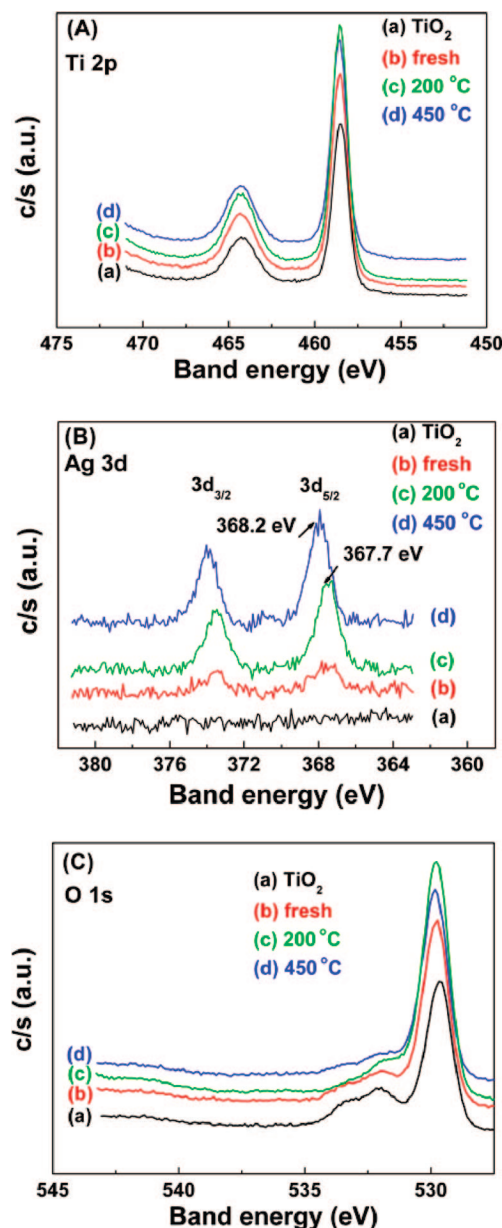


**Figure 4.** XPS spectra of  $\text{TiO}_2$  and  $\text{Ag-TiO}_2$  samples: (A) Ti 2p, (B) Ag 3d, and (C) O 1s. Each spectrum involves (a)  $\text{TiO}_2$  powders, (b) fresh  $\text{Ag-TiO}_2$ , (c)  $\text{Ag-TiO}_2$  heated at 200  $^\circ\text{C}$ , and (d)  $\text{Ag-TiO}_2$  heated at 450  $^\circ\text{C}$ .

$\text{Ag(0)}$  dominate the Ag species within  $\text{Ag-TiO}_2$  and the shift of Ag  $3d_{5/2}$  peak to 368.2 eV (curve d). In addition, from the analysis of curve-fitted O 1s XPS spectra (Figure 4C), similar results could be obtained, as shown in the Support Information (Table S1). These XPS results confirm that  $\text{Ag(0)-TiO}_2$  and  $\text{Ag(I)-TiO}_2$  (mainly  $\text{Ag}_2\text{O-TiO}_2$ ) can be prepared by the PRT method at 450 and 200  $^\circ\text{C}$ , respectively, as shown in eq 1.

**3.2. Photocurrent Actions.** To examine the influence of the chemical states of Ag on the PEC properties of  $\text{Ag-TiO}_2$ , measurements of the photocurrent action spectra were performed in a home-built PEC experimental system. Figure 5 shows the photocurrent action spectra of the  $\text{TiO}_2$ , fresh  $\text{Ag-TiO}_2$ ,  $\text{Ag(I)-TiO}_2$  and  $\text{Ag(0)-TiO}_2$  samples, respectively. As shown, all the samples showed a photocurrent spectrum with the maximum wavelength at about 340 nm corresponding to the band gap of nanocrystalline  $\text{TiO}_2$ , which

(28) Wagner, C. D.; Riggs, W. M.; Davis, L. E.; Moulder, J. F. *Handbook of X-Ray Photoelectron Spectroscopy*; Perkin-Elmer Corp., Physical Electronics Division: Eden Prairie, MN, 1979.

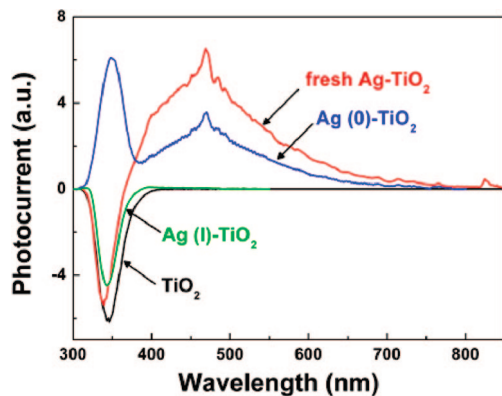


**Figure 5.** Photocurrent action spectra of TiO<sub>2</sub>, fresh Ag–TiO<sub>2</sub>, Ag(I)–TiO<sub>2</sub>, and Ag(0)–TiO<sub>2</sub> electrodes. Photocurrent measurements were done with no bias in the aqueous solution of 0.1 M KNO<sub>3</sub>. Scan rate: 1 nm/s.

was blue-shifted from the band gap of bulk TiO<sub>2</sub> (387 nm, 3.2 eV), mainly due to the size effect of the nanostructure.<sup>29,30</sup> Interestingly, besides the photocurrent generated in UV region, the fresh Ag–TiO<sub>2</sub> and Ag(0)–TiO<sub>2</sub> samples also showed a broad photocurrent spectrum with a notable intensity covering the range of 400–800 nm and the maximum at 470 nm, respectively. However, there was no similar photocurrent response in the range of 400–800 nm for the TiO<sub>2</sub> and Ag(I)–TiO<sub>2</sub> samples.

The above results indicate that the existence of Ag(0) within Ag–TiO<sub>2</sub> resulted in considerable photocurrent response in the range of 400–800 nm. This effect can be attributed to the surface plasma resonance (SPR) effect of Ag(0), whose role is similar to that of a sensitizer in a dye-sensitized solar cell (DSSC).<sup>31</sup> Ag(0) can be excited by visible light in specific wavelengths, and the photoexcited electrons could be further transported to TiO<sub>2</sub> because of the Schottky junction formed at the Ag/TiO<sub>2</sub> interface.<sup>32,33</sup> The electric field in the space charge layer promotes the transport of excited electrons from the Ag/TiO<sub>2</sub> interface to the TiO<sub>2</sub> bulk, and enhances the charge separation between the photoexcited electrons and Ag<sup>+</sup> to facilitate the photo-oxidation of Ag(0). Subsequently, most of the photoexcited electrons could be transported from TiO<sub>2</sub> to the FTO substrate and generate the anodic photocurrent in our case.

In order to further confirm the relation between Ag(0) and the visible light-induced photocurrent, the photocurrent action spectra of Ag(I)–TiO<sub>2</sub> before and after the thermal treatment at 450 °C were investigated. As shown in Figure 6, Ag(I)–TiO<sub>2</sub> had no photocurrent response to the visible light; but after heated at 450 °C, most Ag(I) in Ag(I)–TiO<sub>2</sub> could be thermally reduced to Ag(0) and a notable photocurrent was observed in the range of 400–800 nm. However, the photocurrent response to the visible light could disappear again, when Ag–TiO<sub>2</sub> was reheated at 200 °C. Thus, it was

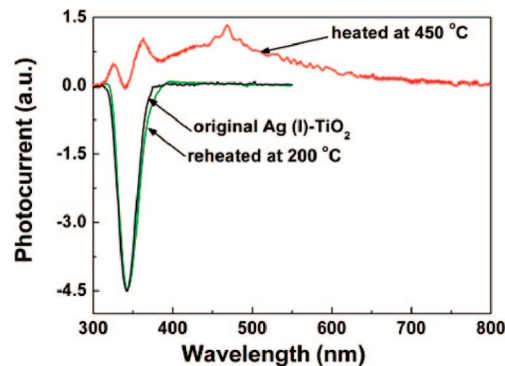


**Figure 6.** Photocurrent action spectra of Ag(I)–TiO<sub>2</sub> electrode with different thermal treatment: original, after being heated at 450 °C, and after being reheated at 200 °C. Photocurrent measurements were done with no bias in the aqueous solution of 0.1 M KNO<sub>3</sub>. Scan rate: 1 nm/s.

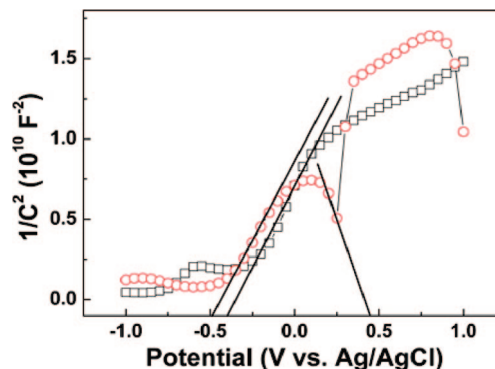


**Figure 7.** Mott–Schottky plots of the Ag(I)–TiO<sub>2</sub> electrode (hollow square) and Ag(0)–TiO<sub>2</sub> electrode (hollow circle). Mott–Schottky measurements were done at the frequency of 1 kHz in the aqueous solution of 0.1 M KNO<sub>3</sub>.

evident that only Ag(0) contributed to the photocurrent in the visible light region, which was due to its SPR effect.

Furthermore, Mott–Schottky (MS) measurements were performed to further characterize the electron transfer properties of the synthesized Ag–TiO<sub>2</sub> nanocomposites. Figure 7 shows the MS plots of the electrodes based on Ag(0)–TiO<sub>2</sub> and Ag(I)–TiO<sub>2</sub>. Reversed sigmoid plots were observed with an overall shape consistent with that typical for n-type semiconductors, and the reproducible flat-band potentials ( $V_{fb0}$ ) could be obtained from the x intercepts of the linear region. Compared with the Ag(I)–TiO<sub>2</sub> electrode, Ag(0)–TiO<sub>2</sub> showed a negative shift in the  $V_{fb0}$  (–0.35 V to –0.5 V), suggesting the presence of more surface states which could lead considerable change in the band position.<sup>29,30</sup> Besides, a notable drop was observed in the plot of Ag(0)–TiO<sub>2</sub> when the applied potential was above 0 V, with the x intercepts of ca. 0.5 V. It was suggested that this effect could be attributed to the generated new surface states in the Ag(0)/TiO<sub>2</sub> interface, which could contribute to the visible light response in the photocurrent action spectrum.

**3.3. Possible Mechanism on the Photocurrent.** Ag(0) rather than Ag(I) has been proved to contribute to the visible light-induced photocurrent by the above results, but there are still two interesting questions: the first one is the stability of Ag(0) in the progress of photocurrent measurement,<sup>31</sup> and the second one is the “reverse” photocurrent of the Ag(0)–TiO<sub>2</sub> electrodes (compared to that of pure TiO<sub>2</sub>) in the UV region. To answer these two questions, a possible

(29) Wang, G.; Wang, Q.; Lu, W.; Li, J. H. *J. Phys. Chem. B* **2006**, *110*, 22029–22034.

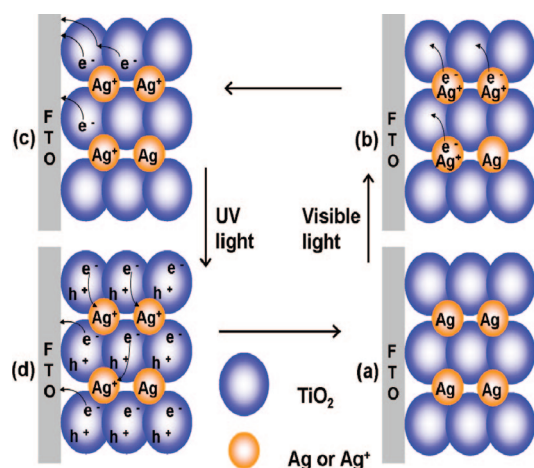
(30) Chen, D.; Wang, G.; Lu, W.; Zhang, H.; Li, J. H. *Electrochem. Commun.* **2007**, *9*, 2151–2156.

(31) Tian, Y.; Tatsuma, T. *Chem. Commun.* **2004**, 1810–1811.

(32) Zhao, G.; Kozuka, H.; Yoko, T. *Thin Solid Films* **1996**, *277*, 147–154.

(33) Kawahara, K.; Suzuki, K.; Ohko, H.; Tatsuma, T. *Phys. Chem. Chem. Phys.* **2005**, *7*, 3851–3855.

**Scheme 1. Transport of Photoexcited Electrons and Interconversion of Ag(0) and Ag(I) by Alternating UV and Visible Light Irradiation during the Photocurrent Action Spectra Measurements<sup>a</sup>**



<sup>a</sup> Pathways: (a to b) Part of the Ag nanoparticles are photoexcited by visible light and the electrons transport to TiO<sub>2</sub> with the formation of Schottky junction; (b to c) photoexcited electrons transport to the FTO substrate via TiO<sub>2</sub> and generate anodic photocurrent with the oxidation of Ag to Ag<sup>+</sup>; (c to d) TiO<sub>2</sub> nanoparticles are excited under UV and the excited electrons transport in two competing ways: to FTO or to Ag<sup>+</sup>; (d to a) part of Ag<sup>+</sup> are reduced to Ag and enter the next cycle.

scheme (Scheme 1) was put forward. In our case, the sample electrode can be irradiated by alternating UV and visible light and undergo two alternating progresses in every cycle of photocurrent measurement. As for Ag(0)–TiO<sub>2</sub>, in the first cycle of measurement, it was in the state shown as Scheme 1a and generated a negative (i.e., “normal”) photocurrent when UV light irradiated (Supporting Information, Figure S1). Followed by the irradiation of the visible light, a part of Ag(0) nanoparticles were photoexcited because of the SPR effect and charge separation was accomplished by the transport of photoexcited electrons from Ag(0) to the TiO<sub>2</sub> conduction band, which finally resulted in the anodic photocurrent in the range of 400–800 nm as well as the simultaneous formation of Ag(I) (b and c in Scheme 1). In the next cycle of photocurrent measurement, TiO<sub>2</sub> nanoparticles in the Ag–TiO<sub>2</sub> electrodes were excited by UV light and the generated photoelectrons would take part in two competing routes (Scheme 1d): (i) transport to FTO glass (or TiO<sub>2</sub>/FTO interface) and generate the negative photocurrent, as in pure TiO<sub>2</sub> electrodes; (ii) transport to the Ag–TiO<sub>2</sub> interface and reduce Ag(I) to Ag(0), which can make Ag–TiO<sub>2</sub> return to the state like (a) (not the same). When route (i) dominated in the UV progress, the Ag–TiO<sub>2</sub> electrode showed a normal photocurrent just like pure TiO<sub>2</sub>; otherwise, a positive (i.e., “reverse”) photocurrent might be observed because lots of electrons moved in a reverse direction (to Ag/TiO<sub>2</sub> interface rather than FTO substrate) and/or the holes rather than electrons acted as the major carriers. From Figure 5, it could be seen that for the fresh Ag–TiO<sub>2</sub>, route (i) dominated in the electron transport progress under UV light, whereas route (ii) played a more important role in the case of Ag(0)–TiO<sub>2</sub> and a “reverse” photocurrent was observed. However, a part of the photo-oxidized Ag(I) (in the form of Ag<sup>+</sup>) would be soon reduced

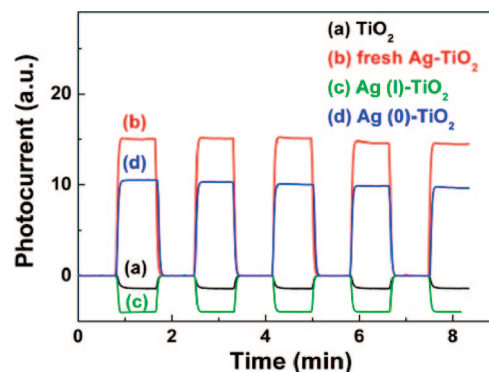


**Figure 8.** Photocurrent response with on-off white light illumination: (a) TiO<sub>2</sub>, (b) fresh Ag–TiO<sub>2</sub>, (c) Ag(I)–TiO<sub>2</sub>, and (d) Ag(0)–TiO<sub>2</sub> electrodes.

to Ag(0) in the following UV irradiation, rather than dissolved in the electrolyte, and would be photoexcited again in the next visible light progress. Thus, in the progress of photocurrent measurements, Ag–TiO<sub>2</sub> electrodes could be irradiated by alternating UV and visible light, and the interconversion of Ag(0) and Ag(I) took place with the alternating light irradiation, which could ensure the stability of Ag and the reproducibility of photocurrent for a relatively long time measurement. This mechanism could explain the above two questions well, but another question rose at the same time, why Ag(I)–TiO<sub>2</sub> electrodes had no response in the visible light region.

According to the Scheme 1, it seems that Ag(I) (Ag<sub>2</sub>O) in Ag(I)–TiO<sub>2</sub> could be reduced to Ag(0) in the UV progress and should generate photocurrent in the following visible light progress. But, the fact is another way. The interconversion between Ag(I) and Ag(0) was inefficient due to the properties of these reactions themselves<sup>22</sup> and the limited time in either progress (ca. several minutes). So in either progress, only a small amount of Ag(0) or Ag(I) could be oxidized (in visible light progress) or reduced (in UV progress), respectively. For Ag(I)–TiO<sub>2</sub>, in the first UV progress, quite few Ag(0) could be generated, and as a result, no notable photocurrent could be observed in the following visible light progress.

To further investigate the photoinduced behavior of the generated photocurrent, the photocurrent response of different samples upon the on-off illumination with white light (xenon lamp, ca. 5 mW/cm<sup>2</sup>) was measured, as shown in Figure 8. When the light was subsequently switched on and off, a series of almost identical signal were obtained. As is well-known that the xenon lamp has a similar energy distribution with sunlight in spectrum, the majority of which consists of the visible and infrared light and only 3–5% of UV light, the electrodes with notable visible light-induced photocurrent suggested high light conversion efficiency and showed much more significant photocurrent because of the effective utilization of visible light. For the fresh Ag–TiO<sub>2</sub> and Ag(0)–TiO<sub>2</sub> electrodes, the photocurrents were 15 and 10 nA, respectively, which was more than three times higher than that of pure TiO<sub>2</sub> and Ag(I)–TiO<sub>2</sub>. It could be concluded that after Ag(0) modification, a much better photovoltaic performance can be achieved under harmless visible light or normal sunlight conditions.



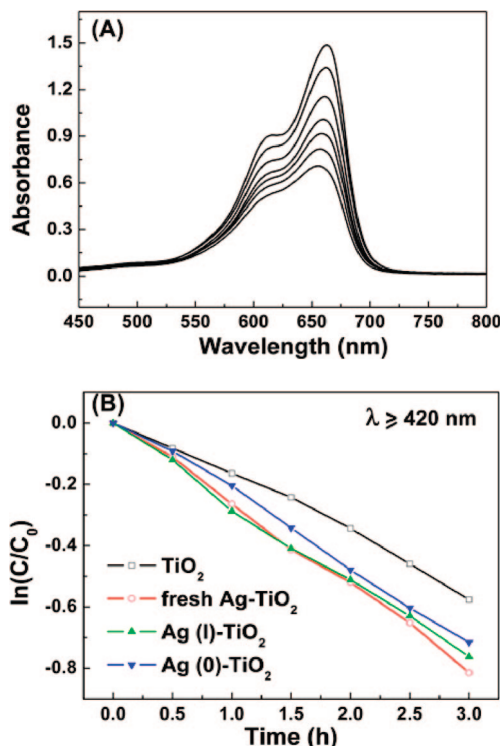


**Figure 9.** (A) UV–visible absorption spectral changes of methyl blue (MB) aqueous solution over the fresh Ag–TiO<sub>2</sub> electrode as a function of irradiation time (xenon lamp:  $\lambda \geq 420$  nm, 30 mW/cm<sup>2</sup>. Curves from top to bottom represent different irradiation time 0, 30, 60, 90, 120, 150, and 180 min, respectively); (B) absorption changes ( $\lambda = 660$  nm) plot for the photocatalytic degradation of MB over TiO<sub>2</sub> (□), fresh Ag–TiO<sub>2</sub> (○), Ag(I)–TiO<sub>2</sub> (▲), and Ag(0)–TiO<sub>2</sub> (▼) electrodes.

**3.4. Photocatalytic Activities.** According to the results of photocurrent action measurements, the Ag–TiO<sub>2</sub> electrodes are expected to show different photocatalytic properties from those of pure TiO<sub>2</sub>, especially under the visible light irradiation. Thus, the photocatalytic activities of fresh Ag–TiO<sub>2</sub>, Ag(0)–TiO<sub>2</sub>, Ag(I)–TiO<sub>2</sub>, and pure TiO<sub>2</sub> electrodes were measured with visible light degradation ( $\lambda \geq 420$  nm) of MB as model reaction and the results are shown in Figure 9. The temporal evolution of the spectra changes accompanying with the photodegradation of MB over the fresh Ag–TiO<sub>2</sub> is shown in Figure 9A. The MB dye initially showed a major absorption band at 660 nm, whereas a gradual decrease in absorption with a slight shift to the shorter wavelengths was observed as the increase of irradiation time, consistent with facile destruction of the chromophoric structure of the MB.

Because the normalized concentration of the MB solution is proportional to the normalized maximum absorbance ( $A$ ),  $A/A_0$  can be replaced by  $C/C_0$ , as shown in Figure 9B. Unexpectedly, Ag(0)–TiO<sub>2</sub> showed poorer photocatalytic activity than fresh Ag–TiO<sub>2</sub> and Ag(I)–TiO<sub>2</sub> though it had notable photocurrent under visible light irradiation. Recently, Ag(0)–TiO<sub>2</sub> obtained by thermal treatment was considered to be inactive in the destruction of azodyes<sup>8</sup> and *E. coli*<sup>20</sup> under visible light, whereas Ag(I) (mainly Ag<sub>2</sub>O) was demonstrated to play an important role in photocatalysis by promoting efficient separation of the generated electrons and holes.<sup>16</sup> In our case, however, it was proposed that both Ag(0) and Ag(I) may be important for the photocatalytic

activities of Ag–TiO<sub>2</sub> nanocomposites, where Ag(0) and Ag(I) could play different roles. On the one hand, Ag(I) could act as active sites for the accumulation of holes, oxygen vacancies and hydroxyl radicals and decrease the recombination of electrons and holes; on the other hand, Ag(0) could play an important role in the stability of Ag–TiO<sub>2</sub> as well as its reproducibility in the photoactivity.<sup>8</sup> Thus, the fresh Ag–TiO<sub>2</sub> which contained both Ag(0) and Ag(I) (though in small amount) showed the best photocatalytic activity among all the samples, and Ag(I)–TiO<sub>2</sub> exhibited higher photocatalytic activity than Ag(0)–TiO<sub>2</sub> under visible light irradiation. However, it should be noted that there are still other factors that influence the photocatalytic activities of Ag–TiO<sub>2</sub> nanocomposites, such as the conversion of Ag(0) to Ag(I) under the visible light during the photocatalysis, which would be further investigated in our future work.

#### 4. Conclusions

In summary, Ag(0)–TiO<sub>2</sub> and Ag(I)–TiO<sub>2</sub> were successfully prepared by the photoreduction-thermal treatment (PRT) method, and their PEC properties were also investigated. The chemical states of Ag introduced a significant effect on the nanocomposites' properties, such as optical properties, electronic properties and PEC properties (including photocurrent actions and photocatalytic activities). It was demonstrated that Ag(0) resulted in the notable photocurrent response to visible light (400–800 nm) because of its SPR effect, and the interconversion of Ag(0) and Ag(I) under alternating UV and visible light irradiation during every cycle of photocurrent measurement ensured the reproducible photoactivity and photostability of Ag–TiO<sub>2</sub>, which can to a great extent facilitate a better use of the visible light and the natural sunlight in the potential PEC applications. In addition, the photocatalytic activities of three types of Ag–TiO<sub>2</sub> under visible light were also investigated. The results indicated that Ag(I) played a more important role than Ag(0) in the photocatalytic degradation by promoting the electron–hole separation and charge transfer, while Ag(0) might be responsible for the photostability of Ag–TiO<sub>2</sub> under visible light irradiation. Thus, for the first time the present work systematically investigated the effect of the chemical state of Ag species on the PEC properties of Ag–TiO<sub>2</sub> nanocomposites. The importance of this study lies in the fact that it revealed the effect of the chemical state of Ag species on the PEC properties of Ag–TiO<sub>2</sub> as well as their corresponding possible mechanisms. Moreover, it also revealed the possibility to achieve better PEC performances of Ag–TiO<sub>2</sub> by tuning the chemical states of Ag species for promising applications in solar energy conversion, photocatalysis, and sensors.

**Acknowledgment.** This work was financially supported by the National Natural Science Foundation of China (20628303), 863 Project (2006AA05Z123), and National Basic Research Program of China (2007CB310500).

**Supporting Information Available:** Table S1 showing the curve fitting of XPS spectra in O 1s region of three types of Ag–TiO<sub>2</sub>; Figure S1 showing the variation of the photocurrent action spectra of Ag(0)–TiO<sub>2</sub> with increasing measurement times (PDF). This material is available free of charge via the Internet at <http://pubs.acs.org>.

CM801796Q